JOURNAL OF MATERIALS SCIENCE 23 (1988) 2064–2068

Intergranular corrosion of welds in type 405 stainless steel

W. J. TOMLINSON, S. J. MATTHEWS
Department of Materials, Coventry Polytechnic, Coventry, CV5 1FB, UK

A low chromium ferritic stainless steel (Type 405) with different heat treatments and weld configurations, has been investigated for susceptibility to intergranular corrosion by chemical and electrochemical potentiodynamic reactivation (EPR) tests, and the results were evaluated by weight losses, dye penetration, metallographic techniques, and the ratio of the reactivating and activating currents. Welds are susceptible to attack, particularly in the heat-affected zone. Applied stress in a U-bend increases significantly the attack on welds, and annealing eliminates the effects of stress. Results on the susceptibility of unwelded specimens in the form of flat plates and U-bends after various heat treatments are also presented and discussed.

1. Introduction

Stainless steels are widely used in chemical and industrial plant because of their excellent resistance to corrosion. The less corrosion resistant ferritic steels, however, are not generally used under such demanding conditions, but the need for greater economies have increased the use of the cheaper ferritic grades. Welding is an important method of fabricating complex plant, and the stability of welds in stainless steel is closely related to the composition of the steel, the thermal conditions associated with welding, and any stress that may be present in service [1–3]. Stainless steels are generally susceptible to intergranular corrosion (IGC) caused by incorrect heat-treatment, and an important case of IGC occurs in the heat-affected zone (HAZ) of welds which, when present, may cause catastrophic failure. Intergranular corrosion of stainless steels is generally considered to be due to zones denuded of chromium which are thereby unable to maintain a passive and protective film of Cr_2O_3 [3]. Depletion of chromium at grain boundaries has recently been measured [4], and it is typically thought to occur by precipitation of chromium carbides [3]. Other mechanisms of intergranular corrosion have been suggested [3]. In particular, it has been considered that local stresses associated with the precipitates are critical [5].

Whilst there has been many studies of IGC in austenitic stainless steel [1–3], there have been only a limited number on the ferritic grades [6, 7]. With the increasing use of welded low-chromium ferritic stainless steels there is a need for more information on the properties of the welded material, and in particular, for information on reliable methods to assess the presence of IGC in such materials. The present work investigates the behaviour of type 405 stainless steel in the unwelded and welded conditions in the form of flat and bent specimens by chemical, electrochemical, and other tests and techniques.

2. Experimental details

Specimens of type 405 stainless steel were commercially obtained in the form of flat coupons and U-bends, each in the unwelded and TIG (no filler metal) welded condition [8]. The specimens had a 180 grit finish with no other post-mill treatment. The chemical analyses are shown in Table I. The microstructure of the as-received material consisted of slightly elongated ferrite grains containing a fine dispersion of carbides. To sensitize the unwelded material, specimens were heated in a helium (99.998% pure) atmosphere for 10 min at 1045° C [9] and then slowly cooled. Some samples were also heated for 1 h at 680° C in air.

Chemical immersion [10] was used to assess the susceptibility to intergranular corrosion. Two tests, ASTM A262-C and A262-E [11], were investigated and finally a modification of A262-E was used. This was based on immersion for 24 h in a boiling solution of $\frac{1}{2}$% H_2SO_4–6% $CuSO_4$–25 g Cu in 500 ml of solution [10]. Analar reagents and distilled water were used. After corrosion, the damage was assessed by weight loss, dye penetration, and standard metallographic techniques. Electrochemical potentiodynamic reactivation (EPR) was also used to assess the susceptibility of the material to intergranular corrosion. In the double-loop variation of the method, the ratio of the current peak on the reverse run to that on the forward run (I_r/I_f) is used as a measure of the degree

TABLE I Chemical composition of the specimens (wt %)

	C	S	Mn	Ni	Cr	Mo	Al	Ti
Flat plate	0.048	0.017	0.51	0.14	13.70	0.016	0.11	< 0.02
U-bend	0.040	0.016	0.39	0.14	13.23	0.036	0.13	< 0.02

0022–2461/88 $03.00 + .12

TABLE II Chemical and EPR corrosion parameters of unwelded type 405 stainless steel in the shape of flat plates and U-bends

Specimen	Condition*	Corrosion test†	Weight loss (mg)	Metallography‡	EPR† (I_r/I_f)	Comments
1	F	Chem	3	No IGA	–	Passed bend test†
2	FH	Chem	376	IGA (2.5)	–	Failed bend test
3	FH	Chem	439	IGA (2)	–	Failed bend test
4	FHR	Chem	45	No IGA	–	Passed bend test
5	FH	EPR	–	–	0.646	
6	FH	EPR	–	–	0.632	
7	FHR	EPR	–	–	0.015	
8	UH	Chem	632	IGA (3.3, 3.2)	–	
9	UH	Chem	–	IGA (3.3, 2.8)	–	
10	UHR	Chem	–	No IGA	–	

*F = flat, U = U-bend, H = sensitization heat-treatment for 10 min at 1045° C, R = relief annealing for 1 h at 680° C.
†See text.
‡Brackets give the mean depth of IGA in μm; with two numbers the first gives the value for the U-bend and the second for the flat region.

of sensitization [12]. In outline, the test consisted of polishing a small sample to a 600 grit finish, soldering to a copper rod, masking with "Lacomit", and then polarizing in 1.5 M H_2SO_4 [13] using a standardized procedure. This consisted of de-aerating 200 ml of solution with nitrogen for 30 min, and then determining the corrosion potential, E_{corr}, of the sample in the solution after 2 min. The specimen was then anodically polarized at 2 mV sec^{-1} to 0.300 V (SCE). At this potential the scan was immediately reversed.

3. Results

Corrosion parameters of the unwelded coupons and U-bends are collected in Table II. We note first that where there has been duplicate tests the quantitative results are very close (see the weight loss and depth of IGA on specimens 2 and 3, the depth of IGA on specimens 8 and 9, and the ratio I_r/I_f on specimens 5 and 6), and thus the procedures give reproducible results. Heat-treatment produced a duplex microstructure of martensite in ferrite, and it was observed that intergranular attack occurred at the martensite/ferrite boundary (Fig. 1). Note also in Fig. 1 that broadening of the martensite/ferrite boundaries has occurred. The integranular attack was not uniform and the depth of attack (Table II) may only be considered an estimate. Typical EPR results are shown in Fig. 2, and the EPR results collected in Table III clearly reveal the susceptibility of the material to IGA (cf. EPR results of specimens 5 and 6 with the data of specimens 2 and 3). Annealing at 680° C eliminated the IGA (specimen 4) and this is also clearly shown in the low EPR value of 0.015 (specimen 7). The U-bends dissolved at nearly twice the rate of the coupons, and the depth of IGA was increased. Annealing at 680° C also eliminated IGA in the U-bends (specimen 10).

Welded specimens in both the flat plate and U-bend forms had a wide range of microstructures and stress

TABLE III Chemical and EPR corrosion parameters of welded type 405 stainless steel

Specimen	Corrosion test*	Weight loss (mg)	Dye* penetrant	Metallography	EPR* (I_r/I_f)
Welded flat plates					
11	Chem	–	No flaws	Slight IGA under weld	–
12	Chem	–	No flaws	Slight IGA under weld	–
13	Chem	4	Small flaws under weld	Cracking under weld	–
14	Chem	4	Small flaws under weld	Cracking under weld	–
15 R†	Chem	–	No flaws	No cracking	
16 R	Chem	34	No flaws	Surface roughening of weld	–
17	EPR	–	–	–	0.040
18	EPR	–	–	–	0.022
19	EPR	–	–	–	0.035
20	EPR	–	–	–	0.017
21	EPR	–	–	–	0.034
Welded U-bends					
22	Chem	–	Fail HAZ + weld	IGA in HAZ + weld	–
23	Chem	–	Fail HAZ + weld	IGA in HAZ + weld	–
24	Chem	–	Fail HAZ + weld	IGA in HAZ + weld	–
25	Chem	34	Fail HAZ + weld	Surface cracking	–
26	Chem	34	Fail HAZ + weld	Surface cracking	–
27 R†	Chem	136	No flaws	Surface etching	–
28	EPR	–	–	–	0.427
29	EPR	–	–	–	0.376

*See text.
†R = relief annealing for 1 h at 680° C.

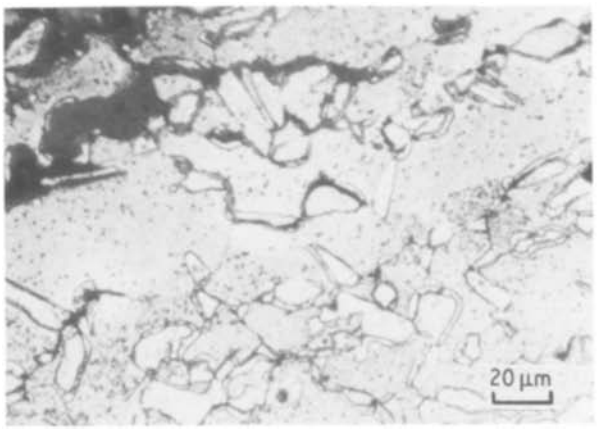

Figure 1 Intergranular attack in type 405 stainless steel sensitized for 10 min at 1045° C. Etched alcoholic ferric chloride.

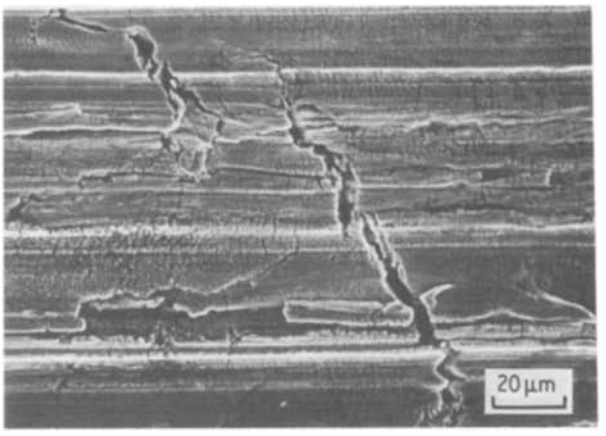

Figure 3 Scanning electron micrograph of the surface of the HAZ of the weld in a U-bend showing intergranular attack.

conditions associated with the weld metal, the HAZ, the bent region of the U-bend, and the as-welded and annealed conditions, and correspondingly there was a wide range of corrosion and/or cracking processes. Results for the welded material are collected in Table III. Overall, there are two general observations. Firstly the damage to the U-bends is much more severe than the damage to the welded flat plate, and secondly, a relief anneal at 680° C eliminates cracking in both the flat plates and in the U-bends.

A consistent feature of the welded U-bends was the deposition of copper from the test solution along the line of the weld, whereas in the flat plate there was merely a general darkening. Extensive damage occurred in the HAZ and, to a lesser extent, in the weld metal of the U-bends. This was of two kinds, typically large-scale IGA (Figs 3 and 4) and much finer cracking normal to the bend stress axis (Figs 3 and 5). The smaller amount of cracking in the weld metal is shown in Fig. 6. Here the filiform corrosive attack is taken to be due to concentration effects in the solution within the cracks. Surface cracks in the welded flat plates were, in contrast to the U-bends, small in number, difficult to locate, and had a quite different morphology (Fig. 7; cf. Figs 3 and 7). In the flat plates no IGA could be found adjacent to or in the weld metal itself although a small amount of IGA was found underneath the weld metal in the HAZ (Fig. 8). Annealing at 680° C tempered the martensite (Fig. 9) which etched preferentially (Fig. 10) and also eliminated IGA (see specimens 16 and 27 of Table III) with corrosion attack in the weld metal being of a more general nature (Fig. 11). EPR results on the U-bends (specimens 28 and 29) show a very poor degree of passivation on the reverse scan, compared with the high degree of passivation indicated by the results on the flat specimens (numbers 17 to 21).

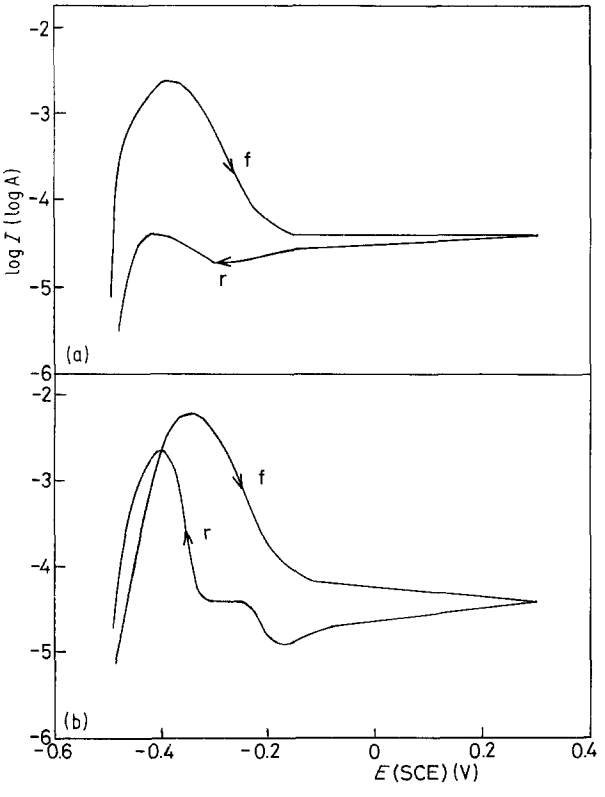

Figure 2 EPR curves showing the forward scan (f) and the reverse scan (r) of a weld in (a) a flat plate (area 20 mm^2) and (b) a U-bend (area 30 mm^2).

4. Discussion

EPR tests differentiate clearly between the IGA characteristics of U-bends and flat plates (Table III), but the weight losses during the chemical tests are misleading. The stresses induced during bending increases the amount of dissolution by ten times (cf. specimens

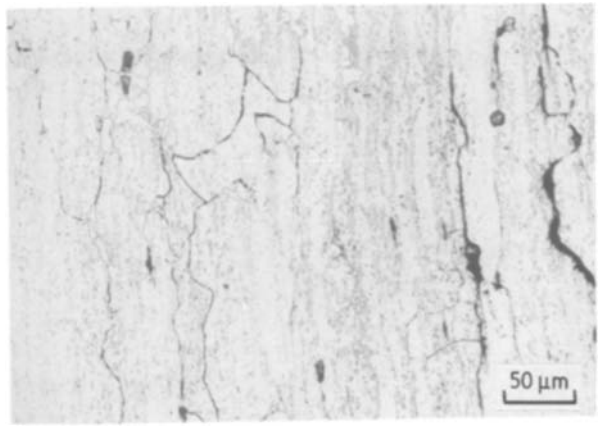

Figure 4 Section of the HAZ of the weld in a U-bend showing intergranular attack. Etched alcoholic ferric chloride.

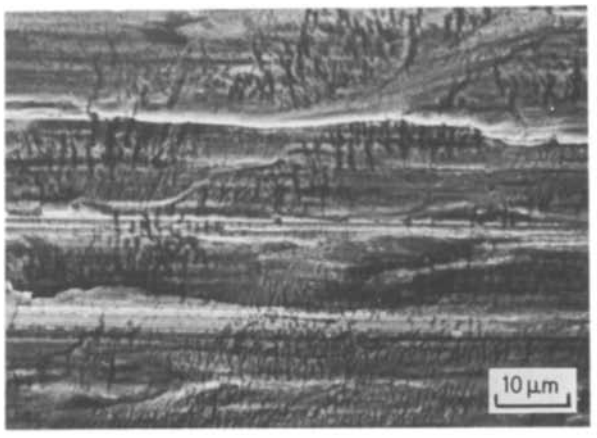

Figure 5 Scanning electron micrograph of fine cracks in the surface of the HAZ of the weld in a U-bend.

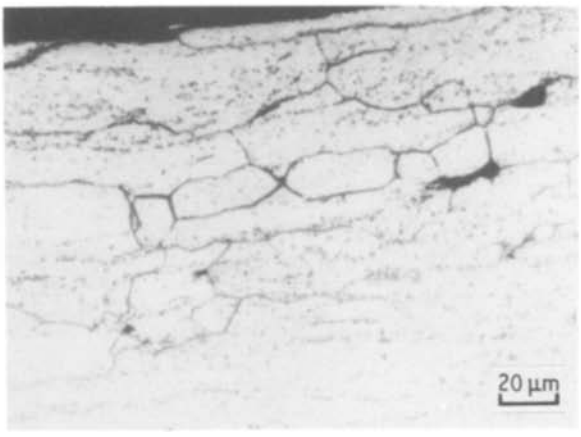

Figure 8 Section of the HAZ of the weld in a flat plate showing intergranular corrosion. Etched alcoholic ferric chloride.

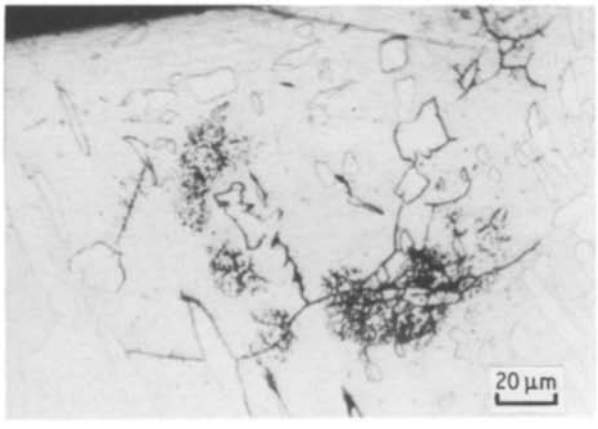

Figure 6 Section of the weld metal in a U-bend. Etched alcoholic ferric chloride.

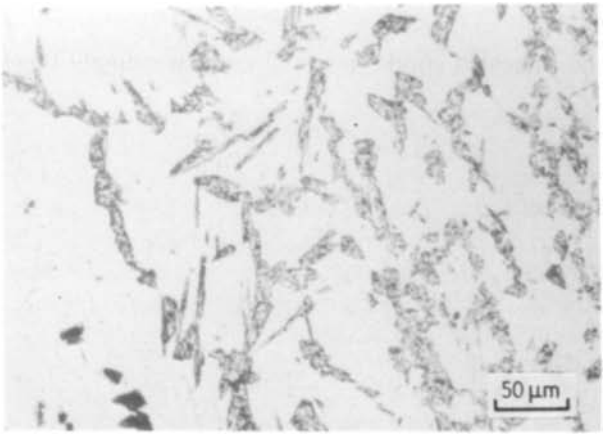

Figure 9 Section of the weld in a flat plate showing tempered martensite. Etched alcoholic ferric chloride.

25 and 26 with 13 and 14, Table III). We note again the accuracy of the duplicate tests and must consider this to be, to a large extent, fortuitous. Annealing at 680° C (specimens 16 and 27) eliminates IGA but increases to amount of corrosion. This is due to general corrosion and not to intergranular attack, because in both cases a noticeable etching or surface roughening occurred. It is clear that this is due to the microgalvanic cells in the tempered martensite (Fig. 9) operating to enhance the corrosion rate [14].

It is difficult with the complex range of structures, stresses and corrosion conditions to identify in detail the processes and mechanisms of failure. In some cases surface corrosion occurs enhanced by the presence of tempered martensite (Figs 9 and 10). But in most cases the attack seems to be essentially intergranular corrosion aided by the residual stress of welding, and more importantly, by the applied stress of bending. It has been suggested that the intergranular attack is due to a chromium depleted zone at grain boundaries, and

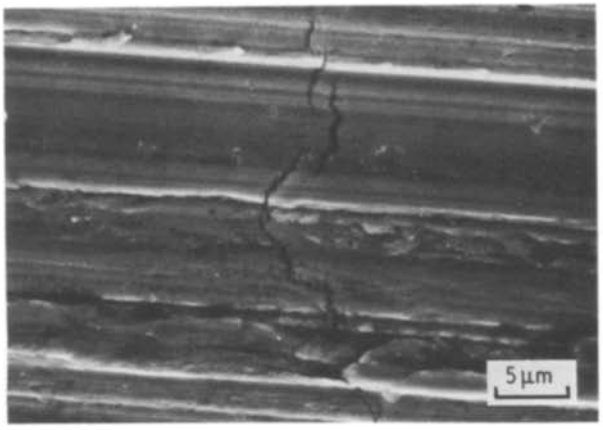

Figure 7 Scanning electron micrograph of the surface cracks in the HAZ of the weld in a flat plate.

Figure 10 Scanning electron micrograph of the surface of the weld metal in a U-bend showing etched surface of tempered martensite.

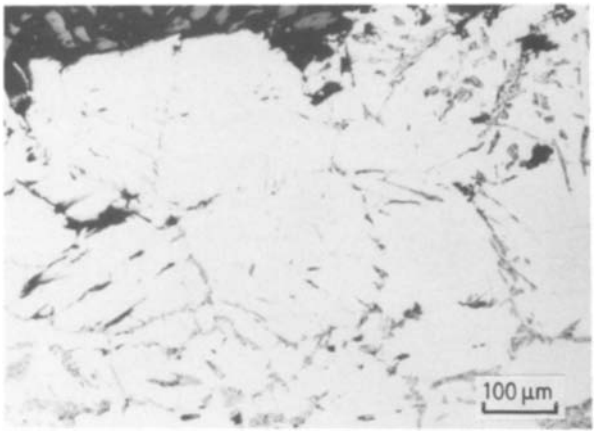

Figure 11 Section of the weld in a U-bend that has been annealed at 680° C. Etched alcoholic ferric chloride.

the present work is entirely consistent with this mechanism. In particular, the precipitation of copper along the weld line must come from an iron-enriched phase to give

$$\underline{\text{Fe}} + \text{Cu}^{2+} = \text{Fe}^{2+} + \text{Cu}$$

and the EPR results indicate the presence of regions difficult to passivate. Stress clearly influences greatly the process and we assume that this is basically by cracking any passivating films. In addition, stress produces a multitude of fine cracks normal to the bend stress axis and within the grains (Figs 3 and 5) which are unrelated to the IGA and appear to be a form of stress corrosion cracking.

5. Conclusions

1. Chemical tests in $\frac{1}{2}\%\ H_2SO_4$–$6\%\ CuSO_4$–25 g Cu (chips), and EPR tests in 1.5 M H_2SO_4 can be used to investigate intergranular corrosion in type 405 stainless steel.

2. Welds in type 405 stainless steel are susceptible to intergranular attack, particularly in the HAZ.

3. Applied stress enhances the intensity of attack in welds. Annealing eliminates the effect of stress.

4. Unwelded specimens of type 405 stainless steel were susceptible to IGA after heat-treatment for 10 min at 1045° C. Further annealing for 1 h at 680° C eliminated IGA.

Acknowledgements

The authors thank British Gas for the supply of materials, and Dr A. J. Jickells of the Midlands Research Station of British Gas for suggesting the project.

References

1. H. H. UHLIG and R. W. WINSTON, "Corrosion and Corrosion Control", 3rd Edn (Wiley, New York, 1985).
2. J. J. DEMO, "Handbook of Stainless Steels" (McGraw-Hill, New York, 1977) pp. 5-1 to 5-40.
3. V. CIHAL, "Intergranular Corrosion of Steels and Alloys" (Elsevier, 1984).
4. J. B. LEE, J. F. SMITH, A. L. GEIGER and D. H. KAH, *Corrosion* **41** (1985) 76.
5. R. A. LULA, A. LENA and G. KIEFER, *Trans. Amer. Soc. Met.* **46** (1954) 197.
6. R. A. LULA and J. A. DAVIS, in "Intergranular Corrosion of Stainless Alloys", ASTM STP 656, edited by R. F. Steigerwald (American Society for Testing and Materials, Philadelphia, Pennsylvania, 1978) p. 233.
7. T. M. DEVINE and B. J. DRUMMOND, *Corrosion* **38** (1982) 327.
8. Metals Samples Company, Inc., RT 1, Box 152, Munford, Alabama 36268, USA.
9. M. A. STREICHER, in "Intergranular Corrosion of Stainless Alloys", ASTM STP 656, edited by R. F. Steigerwald (American Society for Testing and Materials, Philadelphia, Pennsylvania, 1978) p. 3.
10. ASTM G31-72, "Standard Recommended Practice for Laboratory Immersion Corrosion Testing", (American Society for Testing and Materials, Philadelphia, Pennsylvania, 1972).
11. ASTM A262A-E, Recommended Practices for Detecting Susceptibility to Intergranular Attack in Stainless Steel, (American Society for Testing Materials, Pennsylvania, 1986).
12. A. P. MAJADI and M. A. STREICHER, *Corrosion.* **40** (1984) 584.
13. J. B. LEE, *ibid.* **42** (1986) 106.
14. W. J. TOMLINSON and K. GILES, *Corrosion Sci.* **23** (1983) 1353.

Received 23 April
and accepted 6 July 1987